

Interface solitons in quadratically nonlinear photonic lattices

Zhiyong Xu¹, Mario I. Molina², and Yuri S. Kivshar¹

¹*Nonlinear Physics Center, Research School of Physics and Engineering,
Australian National University, Canberra ACT 0200, Australia*

²*Departamento de Física, Facultad de Ciencias, Universidad de Chile, Casilla 653, Santiago, Chile*

We study the properties of two-color nonlinear localized modes which may exist at the interfaces separating two different periodic photonic lattices in quadratic media, focussing on the impact of phase mismatch of the photonic lattices on the properties, stability, and threshold power requirements for the generation of interface localized modes. We employ both an effective discrete model and continuum model with periodic potential and find good qualitative agreement between both models. Dynamics excitation of interface modes shows that, a two-color interface twisted mode splits into two beams with different escaping angles and carrying different energies when entering a uniform medium from the quadratic photonic lattice. The output position and energy contents of each two-color interface solitons can be controlled by judicious tuning of the lattice parameters.

PACS numbers: 42.65.-k, 42.65.Tg, 42.65.Wi

I. INTRODUCTION

Electromagnetic surface waves are waves localized at an interface separating either *two homogeneous* (one of them has to be surface-active, i.e., exhibiting a negative permittivity [1]) or *homogeneous and periodic* dielectric media [2]. In addition, nonlinear dielectric media can support nonlinear guided waves localized at or near the surfaces, and different types of nonlinear guided waves in planar waveguides have been studied extensively about 20 years ago [3, 4]. Recently, the interest in the study of electromagnetic surface waves has been renewed after the theoretical prediction [5] and subsequent experimental demonstration [6] of nonlinearity-induced self-trapping of light near the edge of a one-dimensional waveguide array with self-focusing nonlinearity, that can lead to the formation of a *discrete surface soliton*. A related effect of light localization and the formation of surface gap solitons have been predicted theoretically and observed experimentally for defocusing periodic nonlinear media [7, 8]. In addition, the concept of nonlinear surface and gap solitons has been extended to the case of an interface separating two different nonlinear periodic media [9, 10, 11, 12].

Surface solitons are usually considered for one-frequency modes propagating in cubic or saturable nonlinear media. However, multicolor discrete solitons in quadratically nonlinear lattices have been studied theoretically in both one- and two-dimensional lattices [13, 14, 15, 16] irrespective to the surface localization effects. Only Siviloglou et al. [17] studied discrete quadratic surface solitons experimentally in periodically poled lithium niobate waveguide arrays, and they employed a discrete model with decoupled waveguides at the second harmonics to model some of the effects observed experimentally.

More elaborated theory of one-dimensional surface solitons in truncated quadratically nonlinear photonic lattices, the so-called *two-color surface lattice solitons*, has been developed recently by Xu and Kivshar [18] who analyzed the impact of the phase mismatch on the

existence and stability of nonlinear parametrically coupled surface modes, and also found novel classes of one-dimensional two-color twisted surface solitons which are stable in a large domain of their existence.

The purpose of this paper is twofold. First, we extend the analysis of two-color surface solitons to the case of two semi-infinite photonic lattices with quadratic nonlinearities. We study, for the first time to our knowledge, two-color interface solitons in photonic lattices with quadratic nonlinear response. We analyze the effect of mismatch on the existence, stability, and generation of such novel surface states. Second, for the analysis outlined above we employ two different approaches widely used in the literature: The coupled-mode theory described by the discrete parametrically coupled equations for the fundamental and second-harmonic fields, and also the continuous model with a periodic potential, and demonstrate that both models give the same qualitative results.

The paper is organized as follows. In Sec. II we discuss the two-color interface localized modes in the framework of a discrete model where the interface is modeled by a jump of the propagation constant, assuming that the matching conditions are nearly satisfied for both semi-infinite lattices. Section III is devoted to the analysis of a more general case described by a continuous model with a periodically varying potential. Thus we consider the light beam propagating along the interface between two dissimilar optical lattices imprinted in quadratic nonlinear media. Besides the study of the properties of interface solitons, we demonstrate the manipulation of surface solitons by tuning the lattice and waveguide parameters. Finally, Sec. IV concludes the paper.

II. DISCRETE MODEL

We consider the propagation of light in a one-dimensional photonic lattice of a finite extent imprinted in quadratic nonlinear media, which involves the interaction between fundamental frequency (FF) and second-

harmonic (SH) waves. Light propagation is described by the following coupled nonlinear discrete equations [13, 18]

$$\begin{aligned} i\frac{du_n}{dz} + C_u(u_{n+1} + u_{n-1}) + 2\gamma u_n^* v_n \exp(+i\beta z) &= 0, \\ i\frac{dv_n}{dz} + C_v(v_{n+1} + v_{n-1}) + \gamma u_n^2 \exp(-i\beta z) &= 0, \end{aligned} \quad (1)$$

where u_n and v_n are the normalized amplitudes of the FF and SH waves, respectively, C_u and C_v are the coupling coefficients, γ characterizes the second-order nonlinearity, and β is the effective mismatch between the two harmonics.

We look for stationary two-mode solutions of Eq. (1) in the form, $u_n(z) = U_n \exp(ibz)$ and $v_n(z) = V_n \exp(2ibz - i\beta z)$, where b is the propagation constant, and obtain the nonlinear algebraic equations for the (real) mode amplitudes, U_n and V_n ,

$$\begin{aligned} -b U_n + C_u(U_{n+1} + U_{n-1}) + 2\gamma U_n V_n &= 0, \\ -2b V_n + C_v(V_{n+1} + V_{n-1}) + \beta_n V_n + \gamma U_n^2 &= 0, \end{aligned} \quad (2)$$

where $\beta_n = \beta_1$ on the left side of the interface, and $\beta_n = \beta_2$ on the right side. We solve Eqs. (2) numerically, via the well-known multi-dimensional Newton-Raphson method, using the results of the anti-continuum limit as initial conditions for the algorithm: When $b \gg \text{Max}[\beta_1; \beta_2]$, it is easy to obtain, $V_n \approx b/(2\gamma)$ and $U_n \approx b/\gamma$. Figures 1(a,b) show an example of the simplest interface mode, where the fields propagating along the waveguides are presented as a superposition of the waveguide modes, $U(x) = \sum_n U_n \phi^{(ff)}(x - n)$, where $\phi^{(ff)}(x)$ is the single FF mode centered on guide n ; similarly for $V(x)$. Using the same numerical approach and starting from the anti-continuum limit, we find several other families of two-color localized modes located at the interface. These modes provide a generalization of the surface modes known for truncated one-dimensional lattices located at different distances from the edge, and corresponding to a crossover between the interface and bulk discrete solitons as discussed earlier [19]. In addition, we find novel classes of the so-called interface twisted modes, and an example of such mode is shown in Figs. 1(c,d). In general the spatial profile of these modes are asymmetrical for $\beta_1 \neq \beta_2$.

For given values of C_u , C_v , β_1 , and β_2 , we compute the minimum value of the propagation constant b and the power

$$P = P_u + P_v = \sum_n (|u_n|^2 + 2|v_n|^2), \quad (3)$$

needed to create a localized mode at one of the interface sites. Figures 2(a,b) show examples of P_{\min} curves for two cases. In the first case, when no interface is present, there is no minimum power to generate a localized mode for small values of β . Outside this interval, power increases more or less symmetrically with increase in $|\beta|$. On the other hand, in the presence of an interface

we observe that the generation of an interface localized mode require a finite power, as shown in Fig. 2(b). The numerically-observed stability of these modes seems to be in agreement with the stability results of the continuous model (see section III).

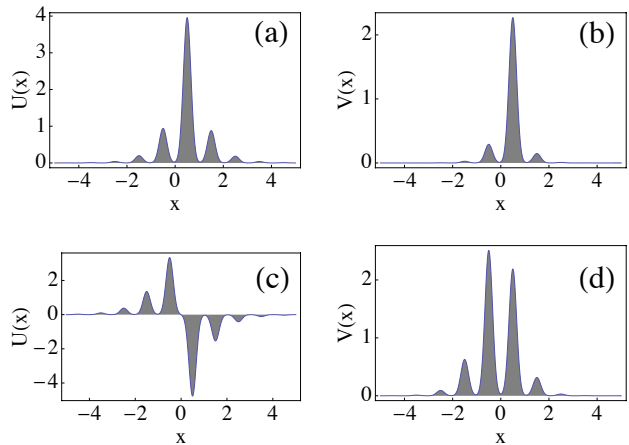


FIG. 1: Examples of two-color interface solitons for $C_u = 1$, $C_v = 0.5$ and (a,b) $b = 5$, $\beta_1 = 3$, $\beta_2 = -3$, and (c,d) $b = 4$, $\beta_1 = 3$, $\beta_2 = -3$. Shown are the amplitudes of the fundamental (a,c) and second-harmonic (b,d) components. Case (a,b) corresponds to a fundamental interface mode, while (c,d) corresponds to an interface “twisted” mode.

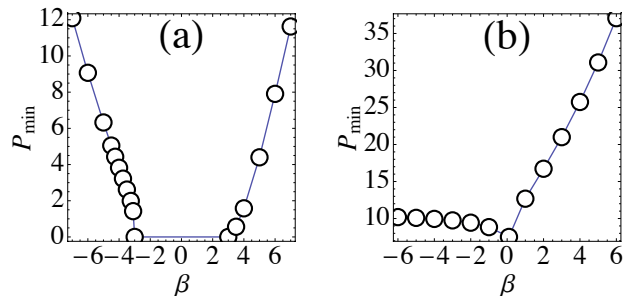


FIG. 2: Minimum power P_{\min} of the simplest two-color interface soliton for $C_u = 1$, $C_v = 0.5$, and (a) $\beta_1 = \beta_2 = \beta$, (b) $\beta_1 = 0$ and $\beta_2 = \beta$.

The dynamical excitation of the interface mode can be achieved by launching all of the initial power in one of the guides adjacent to the interface. When both, FF and SH fields are initially present, a localized mode is formed if the power is strong enough. In the more experimentally relevant case when only the FF field is initially present, the threshold power increases significantly. After the interface mode has been established, the power exchange between the FF and SH fields proceeds along the longitudinal direction with a spatial period that decreases with increasing initial power, for β_1, β_2 fixed. On the other hand, for a fixed value of initial power in the FF field, enough to excite the interface mode, the spatial period

for power exchange between the fields decreases with an increase in the value of $|\beta|$ at the initial launching guide. Figure 3 shows an example of the dynamical excitation of a simple odd mode and a twisted mode, where only the FF field is excited initially. Internal oscillations of the field as well as asymmetrical power sharing for the twisted mode are apparent.

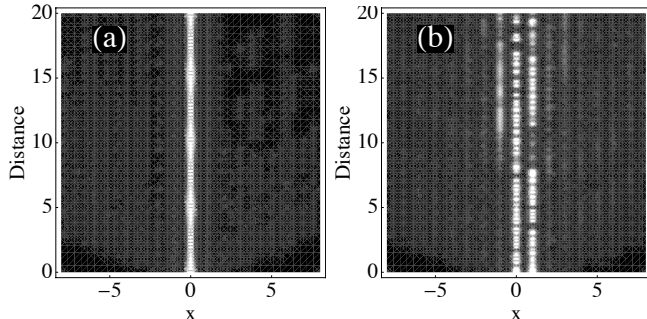


FIG. 3: Dynamical excitation of interface modes. Power content in the FF field for (a) Simple odd mode and (b) Twisted mode. Only FF field is excited initially. Here $C_u = 1, C_v = 0.5, \beta_1 = 3, \beta_2 = -3$.

III. CONTINUOUS MODEL WITH A PERIODIC POTENTIAL

In this section, we extend the analysis to a more general model (a continuous model with a periodically varying potential) to describe propagation of light at the interface between two dissimilar optical lattices imprinted in quadratic nonlinear media, which involves the interaction between fundamental frequency and second-harmonic waves. Light propagation is described by the following coupled nonlinear equations [18]

$$\begin{aligned} i \frac{\partial u}{\partial z} &= \frac{d_1}{2} \frac{\partial^2 u}{\partial x^2} - u^* v \exp(-i\beta z) - pR(x)u, \\ i \frac{\partial v}{\partial z} &= \frac{d_2}{2} \frac{\partial^2 v}{\partial x^2} - u^2 \exp(i\beta z) - 2pR(x)v, \end{aligned} \quad (4)$$

where u and v represent the normalized complex amplitudes of the FF and SH fields, x and z stand for the normalized transverse and longitudinal coordinates, respectively, β is the phase mismatch, and $d_1 = -1, d_2 = -0.5$; p is the lattice depth; the function $R(x) = s[1 - \cos(K_2 x)]$ at $x < 0$ and $R(x) = 1 - \cos(K_1 x)$ at $x \geq 0$ describes the profile of a waveguide array formed with two dissimilar lattices with modulation frequencies K_1 and K_2 , respectively, where s is the relative lattice depth for the left-side one [a typical profile for such tunable waveguide array is shown in Fig. 4]. In typical quadratic nonlinear crystals, for a beam width of $\sim 15\mu\text{m}$, the distance z in the range $0 - 30$ corresponds to a few centimeters, and the peak intensities will be in the range of $0.1 - 10\text{GW}/\text{cm}^2$ for the formation of

lattice solitons at wavelengths $\lambda = 1\mu\text{m}$; a refractive index modulation depth of the order of 10^{-4} corresponds to the lattice depth $p \sim 1$ [18]. The system of Eq. (4) admits several conserved quantities including the power $P = \int_{-\infty}^{\infty} (|u|^2 + |v|^2) dx$.

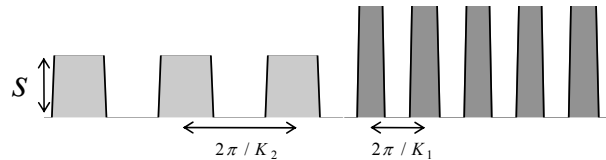


FIG. 4: Interface structure created by two different quadratic lattices with tunable guiding parameters.

The stationary solutions for the lattice-supported interface solitons can be found in the form $u(x, z) = w_1(x) \exp(ib_1 z)$ and $v(x, z) = w_2(x) \exp(ib_2 z)$, where $w_{1,2}(x)$ are real functions, and $b_{1,2}$ are real propagation constants satisfying $b_2 = \beta + 2b_1$. Families of interface solitons are determined by the propagation constant b_1 , the lattice depth p and s , and the phase mismatch β . For simplicity, we set the modulation parameter $K_1 = 4$ and vary K_2 . To analyze stability we examine perturbed solutions $u(x, z) = [w_1(x) + U_1(x, z) + iV_1(x, z)] \exp(ib_1 z)$ and $v(x, z) = [w_2(x) + U_2(x, z) + iV_2(x, z)] \exp(ib_2 z)$, where real parts $U_{1,2}$ and imaginary parts $V_{1,2}$ of perturbation can grow with complex rate δ . The linearization of Eq. (4) around $w_{1,2}$ yields the following eigenvalue problem:

$$\begin{aligned} \delta U_1 &= \frac{d_1}{2} \frac{\partial^2 V_1}{\partial x^2} - (w_1 V_2 - w_2 V_1) - pR V_1 + b_1 V_1, \\ \delta V_1 &= -\frac{d_1}{2} \frac{\partial^2 U_1}{\partial x^2} + (w_1 U_2 + w_2 U_1) + pR U_1 - b_1 U_1, \\ \delta U_2 &= \frac{d_2}{2} \frac{\partial^2 V_2}{\partial x^2} - 2w_1 V_1 - 2pR V_2 + b_2 V_2, \\ \delta V_2 &= -\frac{d_2}{2} \frac{\partial^2 U_2}{\partial x^2} + 2w_1 U_1 + 2pR U_2 - b_2 U_2, \end{aligned} \quad (5)$$

which we solve numerically to find the growth rate δ .

The tunable waveguide array shown in Fig. 4 supports rich families of two-color interface lattice solitons. In semi-infinite waveguide arrays ($s = 0$) the properties of two-color surface solitons have been investigated [18]. Here we are interested in the case $s \neq 0$ thus we can show how to manipulate two-color lattice interface solitons by tuning the lattice and waveguide parameters s and modulation frequency K_2 . The simplest example of a two-color interface mode (odd soliton) is shown in Fig. 5(a), from which one notices that the peak of this mode coincides with one of the maxima of the lattices. As shown in Fig. 5(b) its total power is almost a monotonic function of the propagation constant. It is important to note that the existence domain of two-color interface solitons is determined by the waveguide parameters, thus the cutoff value of propagation constant varies depending on the lattice period [Fig. 5(c)] and depth [Fig. 5(d)]. A lin-

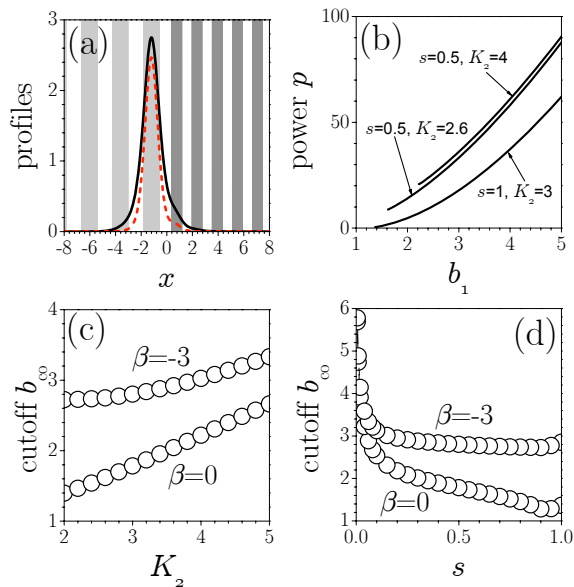


FIG. 5: (Color online) Two-color odd interface solitons (a) FF (black solid curve) and SH (red dashed curve) field distributions of two-color odd interface solitons with $b_1 = 4$ at $s = 0.5$ and $K_2 = 2.6$. (b) Power versus propagation constant for different parameters as marked in the plot, In (a,b) phase matching $\beta = 0$. (c, d) Cutoffs of the propagation constant b_1 versus (c) the lattice period K_2 at $s = 0.5$ and (d) the relative lattice depth s at $K_2 = 3$ for different β .

ear stability analysis reveals that these odd solitons are stable almost in the entire domain of their existence.

Besides the odd solitons described above, we find that the tunable waveguide with two dissimilar optical lattices also supports higher-order interface lattice solitons, which can be viewed as combinations of several odd solitons in engineered phases. Fig. 6(a) shows the case where the FF field features the out-of-phase combination because the in-phase combinations are unstable; we term the mode with an out-of-phase combination as “twisted interface lattice solitons”. There exist cutoff values of propagation constant for twisted interface solitons, which depend on the lattice period [Fig. 6(c)] and lattice depth [Fig. 6(d)]. Note that the profiles of twisted modes are asymmetric due to the dissimilarity of the lattices on two sides [Fig. 6(a)]. An important result is that such asymmetric twisted modes are stable when the power exceeds a critical value [unstable region is shown in dotted curves in Fig. 6(b)], which is confirmed by both, our linear stability analysis and the direct numerical simulation of the soliton generation from the fundamental beam in the framework of the model (4). Generation and stable propagation of asymmetric twisted surface solitons is also shown in Fig. 7(b).

One of the key issues in this paper is to demonstrate the control and manipulation of two-color interface solitons by tuning the guiding parameters of the waveguide array. Removal of the lattices causes each component of the twisted soliton to fly apart because the inter-

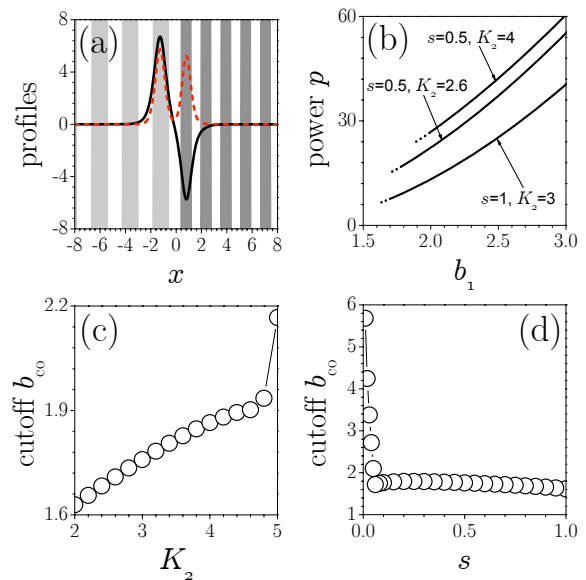


FIG. 6: (Color online) Two-color twisted interface solitons (a) FF (black solid curve) and SH (red dashed curve) field distributions with $b_1 = 4$ at $s = 0.5$ and $K_2 = 2.6$. (b) Power versus propagation constant for different parameters as marked in the plot [Solid and dotted curves correspond to stable and unstable branches, respectively]. (c, d) Cutoffs of the propagation constant b_1 versus (c) the lattice period K_2 at $s = 0.5$ and (d) the relative lattice depth s at $K_2 = 3$. Here phase matching $\beta = 0$.

action force between neighboring constituents is repulsive, due to the out-of-phase combination that forms a twisted mode. Figs. 7(c,d) show a scenario in which a two-color interface twisted soliton splits into two beams carrying different energies when entering into a uniform medium from the quadratic photonic lattices. Note that the power carried by each beam is different due to the lattice-induced asymmetric profiles of two constituents of the twisted solitons and as a result, the escaping angles are different for the two beams. Thus, we can control the output position of the two beams and the power sharing by tuning the guiding parameters of the quadratic photonic lattices. The whole manipulation and switching scenarios of twisted two-color interface solitons in tunable lattices are summarized in Fig. 8, from which one can see clearly that the escape angle and energies of two constituents of twisted solitons can be controlled by tuning the relative lattice depth s [Figs. 8(a,b)] and the modulation frequency K_2 of the lattices [Figs. 8(c,d)]. These results suggest novel opportunities to control the flow of light in tunable photonic systems.

IV. CONCLUSIONS

We have studied parametric localization of light at an interface separating two different quadratically nonlinear photonic lattices and determined the conditions for

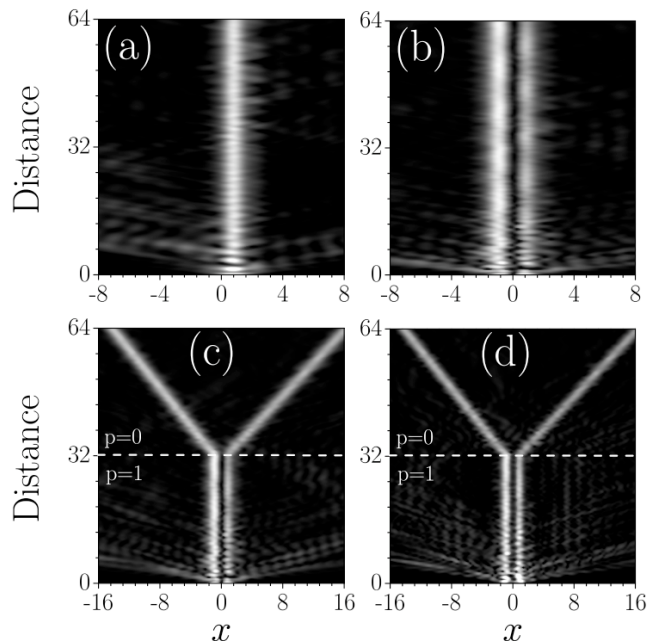


FIG. 7: Excitation of interface solitons from only FF field as input beam: FF field distributions of generated odd (a) and twisted (b) interface solitons. (c,d) Splitting of generated twisted interface solitons at the boundary between a uniform and periodic media for (c) FF and (d) SH fields. Here $\beta = 0$, $s = 0.5$, and $K_1 = K_2 = 4$.

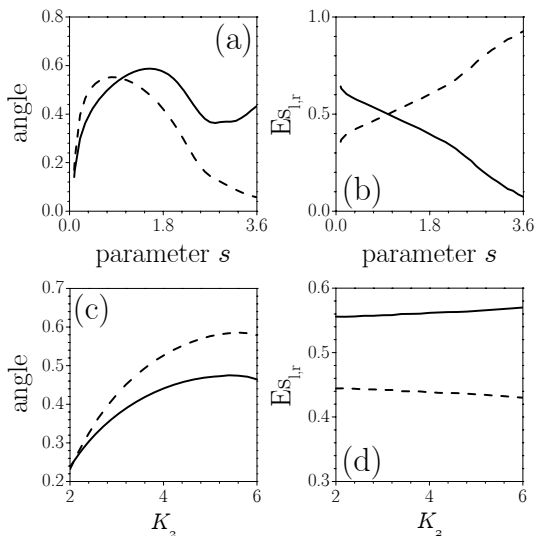


FIG. 8: (a) Escape angles and (b) energy sharing of interface twisted solitons as a function of parameter s for $K_2 = 4$. (c) Escape angles and (d) energy sharing of interface twisted solitons as a function of parameter K_2 at $s = 0.5$. Here Phase matching $\beta = 0$. In all cases solid and dashed curves correspond to the left and right beams in the twisted soliton, respectively.

the existence of interface localized modes. We have analyzed the impact of the phase mismatch on the properties and stability of interface localized modes, as well as the threshold power for their generation. We have employed two different approaches: the coupled-mode theory and a continuous model with a periodic potential. Both models give basically the same qualitative results. Our results reveal that asymmetric phase-twisted two-color surface solitons are stable in a broad region of system parameters, but they can split into two solitons when entering a homogeneous medium. We have demonstrated that the output position and energies of constituents of the two-color interface solitons can be controlled by tuning the lattice and waveguide parameters.

V. ACKNOWLEDGEMENTS

This work was supported by Fondecyt grant 1080374 and by the Australian Research Council.

[1] G. Borstel and H.J. Falge, in: *Electromagnetic Surface Modes*, Ed. A.D. Boardman (Wiley, Chichester, 1982).

[2] P. Yeh, A. Yariv, and A.Y. Cho, *Appl. Phys. Lett.* **32**,

- 104 (1978).
- [3] See, e.g., D. Mihalache, M. Bertolotti, and C. Sibilia, *Prog. Opt.* **27**, 229 (1989), and references therein.
- [4] A.D. Boardman, P. Egan, F. Lederer, U. Langbein, and D. Mihalache, in: *Nonlinear Surface Electromagnetic Phenomena*, V.M. Agranovich, A.A. Maradudin, H.-E. Ponath, and G.I. Stegeman, eds. (Elsevier Science Publishers B.V., New York, 1991), pp. 73-287.
- [5] K.G. Makris, S. Suntsov, D.N. Christodoulides, G.I. Stegeman, and A. Haché, *Opt. Lett.* **30**, 2466 (2005).
- [6] S. Suntsov, K.G. Makris, D.N. Christodoulides, G.I. Stegeman, A. Haché, R. Morandotti, H. Yang, G. Salamo, and M. Sorel, *Phys. Rev. Lett.* **96**, 063901 (2006).
- [7] Ya.V. Kartashov, V.V. Vysloukh, and L. Torner, *Phys. Rev. Lett.* **96**, 073901 (2006).
- [8] C.R. Rosberg, D.N. Neshev, W. Krolikowski, A. Mitchell, R.A. Vicencio, M.I. Molina, and Yu.S. Kivshar, *Phys. Rev. Lett.* **97**, 083901 (2006).
- [9] K.G. Makris, J. Hudock, D.N. Christodoulides, G.I. Stegeman, O. Manela, M. Segev, *Opt. Lett.* **31**, 2774 (2006).
- [10] K. Motzek, A.A. Sukhorukov, and Yu.S. Kivshar, *Opt. Exp.* **14**, 9873 (2006).
- [11] M.I. Molina and Yu.S. Kivshar, *Phys. Lett. A* **362**, 280 (2007).
- [12] S. Suntsov, K.G. Makris, D.N. Christodoulides, G.I. Stegeman, R. Morandotti, M. Volatier, V. Aimez, R. Ares, E. H. Yang, and G. Salamo, *Opt. Express* **16**, 10480 (2008).
- [13] B.A. Malomed, P.G. Kevrekidis, D.J. Frantzeskakis, H.E. Nistazakis, and A.N. Yannacopoulos, *Phys. Rev. E* **65**, 056606 (2002).
- [14] Ya.V. Kartashov, L. Torner, and V.A. Vysloukh, *Opt. Lett.* **29**, 1117 (2004); Ya.V. Kartashov, V.A. Vysloukh, and L. Torner, *ibid.* **29**, 1399 (2004).
- [15] Z. Xu, Ya.V. Kartashov, L.-C. Crasovan, D. Mihalache, and L. Torner, *Phys. Rev. E* **71**, 016616 (2005).
- [16] H. Susano, P.G. Kevrekidis, R. Carretero-Gonzalez, B.A. Malomed, and D.J. Frantzeskakis, *Phys. Rev. Lett.* **99**, 214103 (2007).
- [17] G.A. Siviloglou, K.G. Makris, R. Iwanow, R. Schiek, D.N. Christodoulides, G.I. Stegeman, Y. Min, and W. Sohler, *Opt. Express* **14**, 5508 (2006).
- [18] Z. Xu and Yu.S. Kivshar, *Opt. Lett.* **33**, 2551 (2008).
- [19] M. Molina, R. Vicencio, and Yu. S. Kivshar, *Opt. Lett.* **31**, 1693 (2006).